JPE 9-6-15

Development of Hybrid Electric Compressor Motor Drive System for Hybrid Electrical Vehicles

Tae-Uk Jung†

†Department of Electrical Engineering, Kyungnam University, Masan, Korea

ABSTRACT

This paper presents a design optimization process for interior permanent magnet synchronous motors (IPMSM) for hybrid electric compressors (HEC) which are applied to hybrid electrical vehicles. A hybrid electric compressor is composed of an electric motor driving section and an engine driving section which is connected to the engine by a pulley belt. A hybrid electric compressor driving motor requires half of the full driving power of a compressor. Even though an engine is not operated at the idling stop mode, the electric motor drives the air-conditioner compressor by itself so that the air conditioning system can produce its minimum cooling capacity. In this paper, the design optimization of an IPMSM for a 42 (V) applied voltage system is studied using the design of experiment (DOE) and response surface method (RSM) of 6sigma. The driving characteristics of this motor drive system are measured and analyzed by experiment.

Keywords: Hybrid electrical vehicle, Hybrid electric compressor, IPMSM, Design optimization

1. Introduction

Recently the development of next generation vehicles which are more efficient and have less air pollution is being carried out actively throughout the world. This next generation vehicle development is divided in two directions; hybrid electrical vehicles (HEV) and fuel cell electrical vehicles (FCEV) [1].

The HEV is being commercialized because of its high fuel efficiency and low air pollution. It is forecasted by economists that the HEV market will expand extensively and it is predicted to be 7% of the new vehicle market share in 2010.

Manuscript received April. 30, 2009; revised Oct. 7, 2009.
† Corresponding Author: tujung@kyungnam.ac.kr
Tel: +82-55-249-2628, Fax: +82-55-249-2839, Kyungnam Univ.
Dept. of Electrical Engineering, Kyungnam University, Korea

Thus, research concerning motor drive systems for HEV, especially the power train motor, is actively being carried out. The highest output power system, except the traction motor, is the air conditioner compressor in a HEV system.

Since the engine is turned off during idle stop mode in a HEV system, a conventional air conditioner can not operate during this period. In the summer this causes the temperature inside a car to rise. Therefore an electric driving type compressor system is necessary in HEV [2-4].

Generally, electric compressors are classified as one of two types. One is a full electric compressor (FEC) and the other is a hybrid electric compressor (HEC).

In a FEC, the driving motor should be large enough to charge the full load power of a compressor and the load burden on the battery is high. On the other hand, a typical HEC driving motor requires half the power of a FEC

because the rated output power is equally imposed on both the motor and the engine. Since the electric motor drive system charges the cooling capacity by itself during idle stop, a hybrid electric motor is a more economical and practical solution [5].

In this paper, an interior permanent magnet synchronous motor (IPMSM) is adopted as a HEC driving motor because it has high efficiency and high output power density characteristics. The design analysis was done by the lumped parameter method (LPM) and a 2D finite element analysis (FEA). Design optimization is accomplished based on the design of experiment (DOE) and response surface method (RSM) of 6sigma.

The driving performance of this motor drive system is measured and verified by experiment.

2. Hybrid Electric Compressor Motor System

A HEC system is configured as shown in Fig.1. In a conventional mechanical compressor system as shown in Fig. 1 (a), the compressor is driven by the engine torque via a pulley belt, and the compressor cannot be operated during the idle stop mode of the HEV. This is the weak point of the mechanical compressor system when applied to a HEV. As a result of this weakness the fuel saving effect would be limited in the summer.

As shown in Fig. 1(b), a HEC is composed of an electric motor driving section and an engine driving section connected to the engine by a pulley belt.

Due to this driving mechanism, the driving torque of the HEC is the sum of the electric motor power and the engine power.

Fig. 2 shows the operation modes of the HEC applied to the air-conditioner of a HEV.

During full power operation mode when a HEV is running, both the engine power and the electric motor rotate the compressor at the same time. During minimum power operation, when the engine is idly stopping, only the electric motor drives the compressor and a minimum of cool air is supplied to the inside of the car. As a result, the air-conditioner can always provide cooling air to the inside of a HEV.

In general, a HEC driving motor requires half of the full driving power of a compressor.

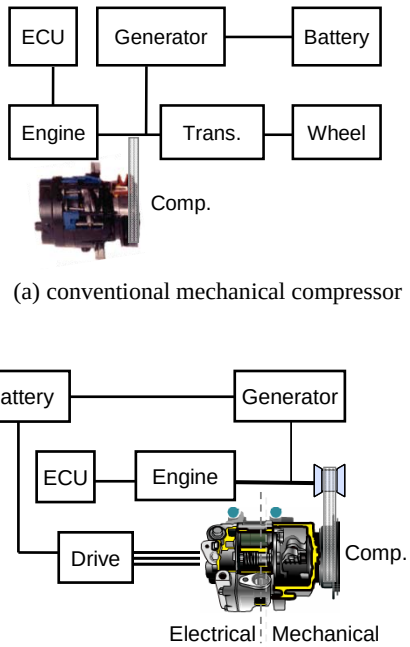

(a) conventional mechanical compressor

(b) HEC (Hybrid Electric Compressor)

Fig. 1. System configuration of air-conditioner compressor.

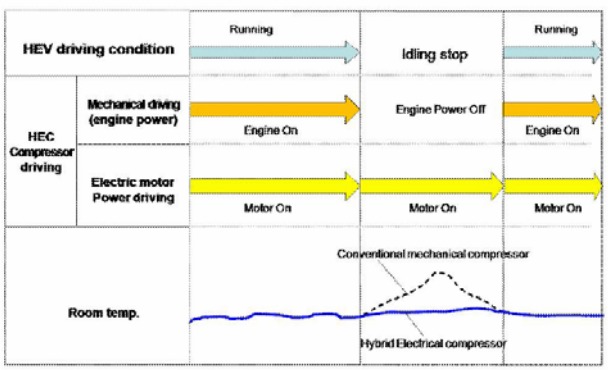

Fig. 2. Operation mode of HEC in HEV.

Generally the full power of a compressor is nearly 4kW, so a HEC driving motor's power can be designed as 2kW.

3. Motor Design Optimization

3.1 Motor Design Procedure

In this study, an IPMSM is adopted as a compressor driving motor due to its high output power and high efficiency under low applied voltage conditions. The design procedure is shown in Fig. 3.

As shown in Fig. 3, the motor's specifications are

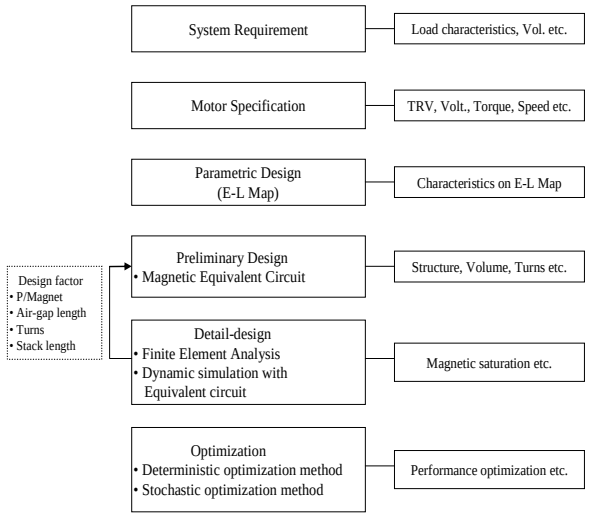

Fig. 3. Design process of electromagnetic structure.

designed by first considering the system's requirements. Then, the dominant design factors range is selected by an E-L map. This E-L map plots the correlation between the back EMF E and the inductance L in accordance with the output power requirements. After that, the preliminary design is executed on the basis of the designed E-L map. Finally, design optimization is accomplished by the DOE and RSM which are design optimization tools of 6sigma.

3.2 System Requirement Design

Table 1 shows the system requirement specifications.

In this study, the applied voltage of the battery is set to 42 (V), and the HEC driving motor's power is designed as 2 (kW); which is half of the full compressor driving power 4 (kW) as explained in Ch. 2.

Table 1. System requirements.

Item	Unit	Specification
System voltage	V	42
Stator out diameter	mm	100.4
Rotor out diameter	mm	48.4
Stack length	mm	<100
Rated output	W	2,000
Rated speed	rpm	3,500
Rated torque	Nm	5.5
Efficiency	%	Over than 90
Operating speed range	rpm	500~7,500
Cooling method		Suction coolant cooling

A higher current is needed for the required output power under a low voltage system such as 42(V). In an optimal design to minimize the applied current it is necessary to acquire high efficiency and high output power density.

3.3 Motor Design Optimization

3.3.1 Design of Torque Per Unit Rotor Volume

In the application of an IPMSM, the typical value of TRV (Torque per unit Rotor Volume) is set within a range of 14~42 (kNm/m^3) in compliance with the air-ventilation cooling condition [6].

This TRV value depends on the cooling method; such as enforced ventilation or natural circulation. The TRV can be designed to be greater than 50 (kNm/m^3) when water cooling is applied.

In this study, the TRV is fixed at 30 (kNm/m^3) taking into consideration the cooling condition; the motor is cooled by the suction of coolant through the compressor.

3.3.2 Preliminary Design

In an IPMSM, the back EMF E and inductance L are crucial design factors for determining output performance and efficiency characteristics.

E-L Mapping is applied to determine the appropriate design scope of these important design variables. In the beginning, the design condition is set up. The output and input characteristics are calculated by the LPM (Lumped Parameter Method) using equivalent circuit characteristics equations employing the design condition. Then they are plotted in the E-L coordinate scale. The best point extracted from the plot is used as the initial value for the preliminary design.

The design conditions are as follows:

a) Inductance difference ratio (saliency) L_q/L_d : over 1.5

b) Rated output and speed : refer to Table 1

c) Mechanical loss : 0.5% of output

d) Phase resistance : 10 mΩ at 120℃

e) Core loss : neglected

Where, L_q is the maximum inductance of the q-axis and L_d is the minimum inductance of the d-axis.

The selected value of each parameter in the E-L map is assessed to meet the system requirements of Table 1. The maximum efficiency point, which is appointed by the E-L

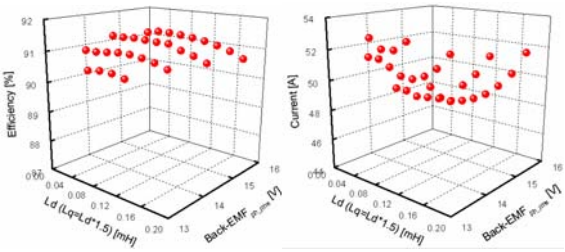

(a) efficiency (b) current

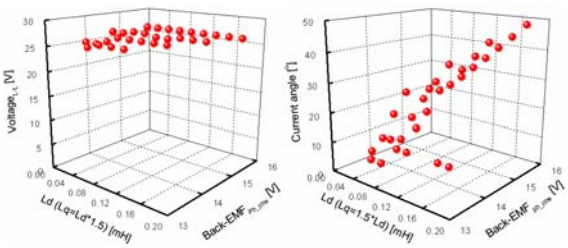

(c) voltage (d) current angle

Fig. 4. Design area selection by E-L Map.

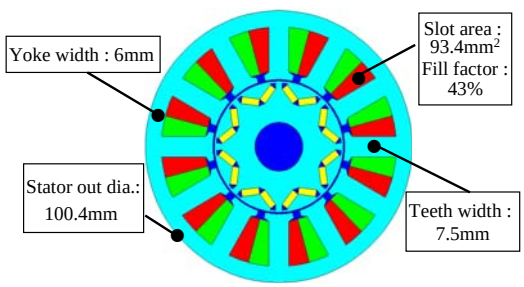

(a) stator

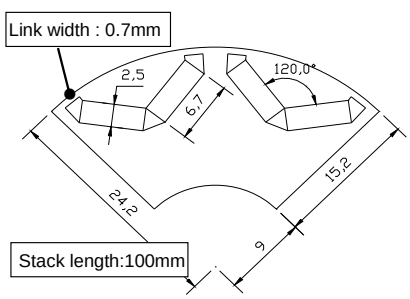

(b) rotor

Fig. 5. Preliminary design structure.

map, is shown in Table 2. It has nearly a 91.1% efficiency characteristic. On the basis of this maximum efficiency point, the preliminary motor structure is designed by FEA to meet the system requirements of Table 1.

The applied voltage of this study is 42V. At this low voltage, a lower BEMF is advantageous for high speed rotation and high saliency is good for high output power density. Therefore, in the preliminary motor structure design, BEMF and saliency are adjusted from the maximum efficiency point. The BEMF is lowered to 14.25 (V) and saliency is increased to 1.63. The preliminary design model's efficiency is still over 90% which is a requirement of Table 1. The preliminary motor structure and the designed parameters are shown in Fig. 5 and Table 2.

Table 2. Preliminary designed parameters.

Items	E-L Map		
	Parameter range	Max. efficiency point	Initially designed value
D-axis Inductance, Ld	0.01 ~ 0.2mH	0.09mH	0.099
BEMF(phase) @3500rpm	13 ~ 16V	15.4V	14.25V
Saliency (Lq/Ld)	1.5	1.5	1.63
Current	47 ~ 53A	48A	48A
Current Phase Angle	0 ~ 50 deg.	28 deg.	28 deg.
Efficiency	over 90%	91.2%	90.6%

This preliminary model is a base structure model and a starting point for design optimization.

3.3.3 Optimization

Design optimization is accomplished by the DOE (Design of Experiment) and RSM (Response Surface Method) as shown in Fig. 6. The DOE is very useful for finding the dominant and critical design factors that influence performance characteristics. At the next step the design is optimized by the RSM to satisfy the required design objectives.

An objective of this design optimization is to minimize cogging torque and torque ripple.

At first, the stator slot opening, the flux barrier angle and the chamfer dimension are selected as main design factors for cogging torque and torque ripple.

a) Cogging torque reduction

Cogging torque is caused by reluctance variation of the permanent magnet flux of a rotor without stator winding excitation. It depends on rotor angular position.

DOE is applied to find the dominant factors for cogging torque. The cogging torque is calculated by 2D FEA

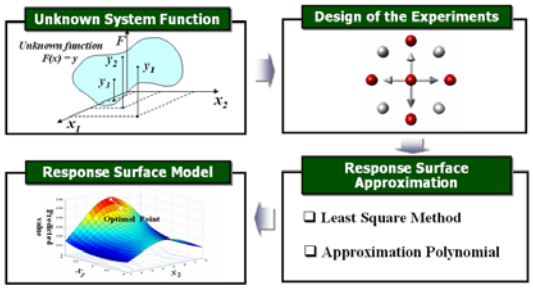

(a) optimization process

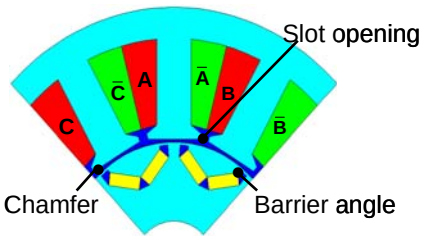

(b) main design factors

Fig. 6. Design optimization procedure.

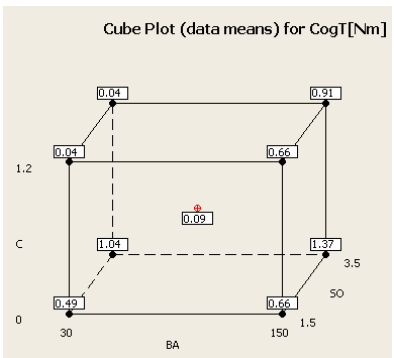

Fig. 7. DOE and cube plot related to the cogging torque.

and written in the boxes in Fig. 7.

Fig. 7 shows the cube plot for the DOE concerning 3 factors and 2 levels. Where, "SO" is the slot opening, "BA" is the barrier angle and "C" is the chamfering value. Each vertex of the cube plot represents the calculated results respectively when the design parameters are combined with each other.

In this cube plot, the center point means the calculated result when the three variables are located at the center of those ranges. For example, in Fig. 7, the center point value 0.09 is the calculated result when C is 0.6 (mm), BA is 90 (deg.) and SO is 2.5 (mm).

These calculated results are also plotted in the Main Effect Analysis graphs in Fig. 8. In Fig. 8, the slope reflects the effectiveness of each parameter. For instance,

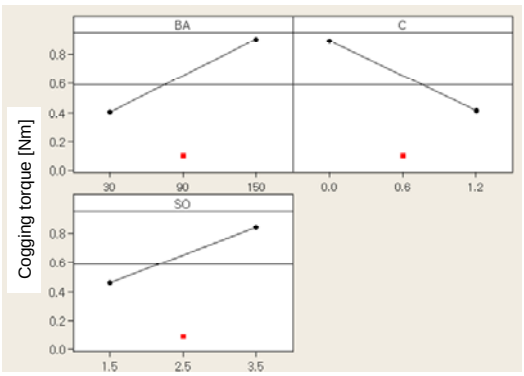

Fig. 8. Main effect analysis for cogging torque.

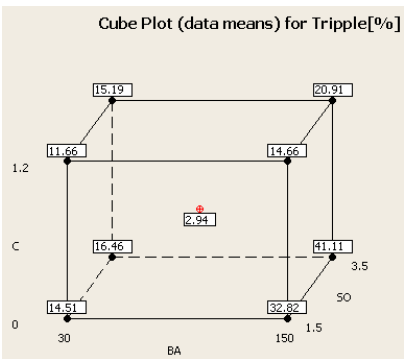

Fig. 9. DOE and cube plot for torque ripple.

a steep slope is ascribed to a large effect in that parameter. As a result, we can see that all three parameters are dominant factors for cogging torque. As a result smaller values of these parameters favor cogging torque reduction.

b) Torque ripple reduction

Instantaneous torque variation is called torque ripple, which causes vibration and acoustic noise in motors.

The design value combination of the DOE is set up as a cube plot in Fig. 9. The torque ripple of each combination of eight vertexes in Fig. 9 is calculated, and written in the boxes.

These calculated results are also plotted in the Main Effect Analysis graphs in Fig. 10.

As a result, all three parameters represent dominant factors for cogging torque, and smaller values of these parameters are beneficial for low torque ripple. However, the slot opening has a negligible effect in comparison with the other parameters.

c) Optimal design by the RSM

As shown in Fig. 8 and Fig. 10, the slot opening should

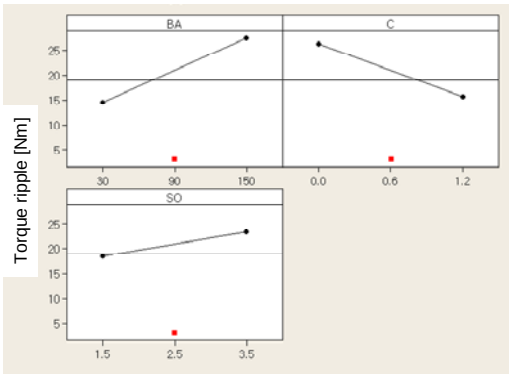

Fig. 10. Main effect analysis for torque ripple.

be minimized to reduce cogging torque and torque ripple. However, the process ability of a winding machine should be considered as well.

In this paper, the slot opening is equal to 1.9 (mm) which is the minimum opening size according to the winding machine's requirements.

In this condition, the optimal design areas of the barrier angle and the chamfer dimension satisfying the three target characteristics written in the right box of Fig. 11 are derived from the RSM.

In Fig. 11, the optimal design areas are selected. They are the two optimal areas A and B. In these two areas, the left optimal area is selected as the optimal design area because the smaller BA (barrier angle) will make the rotor more robust from the viewpoint of mechanical strength.

In the left optimal area A, the torque ripple T_{ripple} is nearly 6%. It is a relatively large value in the design value range 4~6%. As the chamfer dimension C is increased, the torque ripple T_{ripple} becomes small. However, the low T_{ripple} range, nearly 4%, is out of the optimal area A.

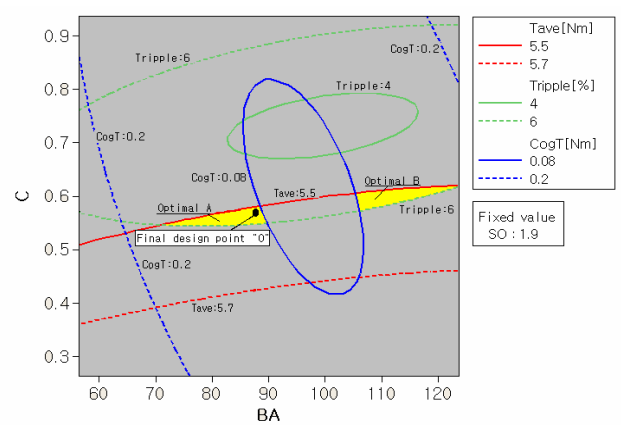

Fig. 11. Optimal design area by RSM.

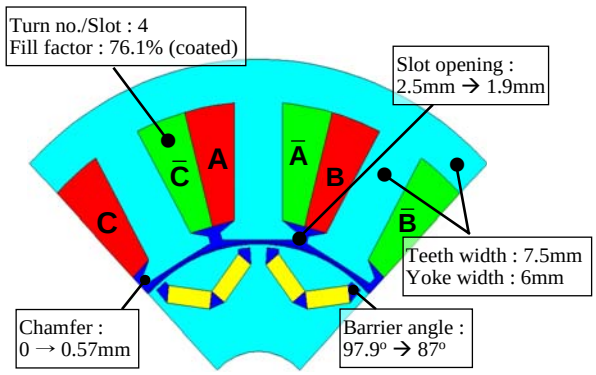

Fig. 12. The structure of final design.

As the optimal design point is lowered, the average torque T_{ave} is increased but the T_{ripple} is also increased. Considering these opposite characteristics of the T_{ave} and the T_{ripple}, the optimal final design point "O" is set where the barrier angle BA is 87 (deg.) and the chamfer dimension C is 0.57 (mm).

Therefore, final design structure and specifications are shown in the Fig. 12 and Table 3, respectively.

Table 3. Final design specification.

Item	Unit	Value
Pole numbers		Stator : 8, Rotor : 12
Stator out diameter	mm	100.4
Rotor out diameter	mm	48.4
Air-gap length	mm	0.6
Stack length	mm	90
Permanent magnet		NdFeB 42AH (Br = 1.16 T @ 120℃, μ_r = 1.05)
Silicon steel		S18
Winding turns / slot	turn	16 (ϕ0.8 x 23 parallel)
Winding fill factor	%	76.1
Phase resistance	mΩ	7.55 (@ 120℃)

Fig. 13 shows the improved result of the cogging torque and the torque ripple derived from the design optimization. These results are simulated using 2D FEA.

4. Motor Design Optimization

The prototype of an IPMSM motor drive system and the air-conditioning test system are implemented as shown in Fig. 14.

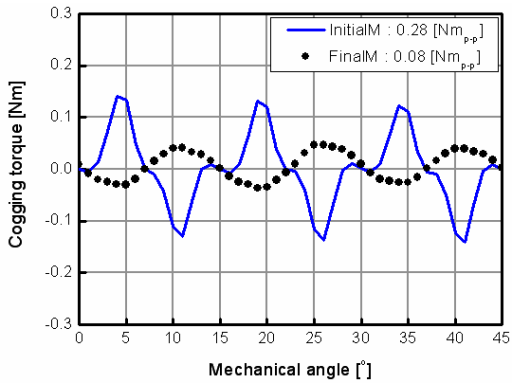

(a) cogging torque

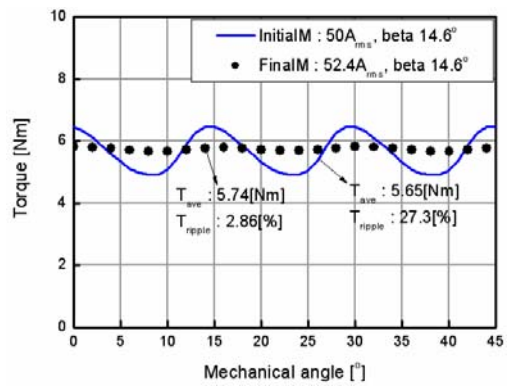

(b) torque ripple

Fig. 13. Comparison of cogging torque and torque ripple between initial model and optimized final model.

(a) stator and rotor of prototype motor

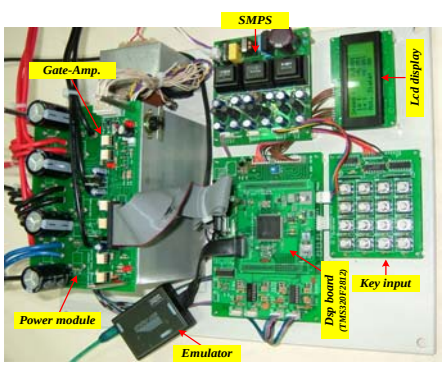

(b) inverter drive

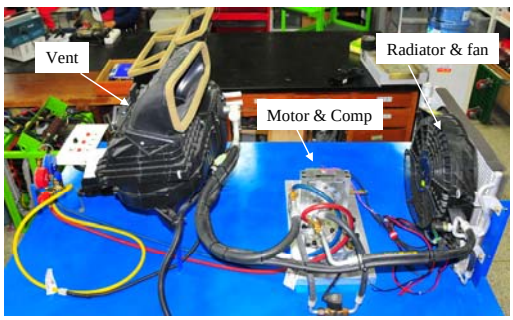

(c) test system

Fig. 14. Prototype of motor, inverter drive and HVAC test system.

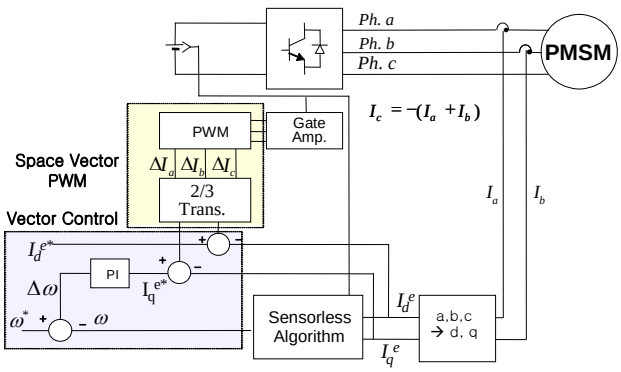

Fig. 15. Block diagram of inverter drive.

The considering point of the inverter circuit design is the large current switching commutation under low voltage 42 (V). A MOSFET is selected as a high frequency switching power device; and two MOSFETs are connected in parallel to commutate a high current.

A DSP TMS320F is used as a control processor, and the peripheral circuit is designed accordingly. Fig. 15 represents a system block diagram of the inverter drive controller.

The driving performance of this motor drive system is measured by a dynamometer.

The driving performance at the rated load is shown in Table 4, and the efficiency characteristic with respect to the load torque variation is shown in Fig. 16. A high efficiency characteristic, over than 90%, was obtained in the experimental test.

Fig. 17 shows the torque ripple characteristics. The torque ripple is within ±6% of the rated torque, and it is within the required torque ripple range of Fig. 11.

Fig. 17 shows the instantaneous torque waveform of the

prototype motor.

Table 4. Rated driving characteristics (3,500 RPM).

Items	Unit	Specification	Remarks
Phase EMF	V	13.4	@3500 rpm
Cogging torque (peak to peak)	Nm	0.08	
Copper loss	W	62.1	
Iron loss	W	102.1	
Mechanical loss	W	61.3	
Efficiency	%	90.0	
Power factor	%	89.9	
D-axis inductance, L_d	mH	14.3	
Q-axis Inductance, L_q	mH	9.6	
Terminal Volt.	V	26.7	
Current	A	52.4	
Current phase angle	degree	14.6	
Torque (simulation)	Nm	5.50	@3500 rpm

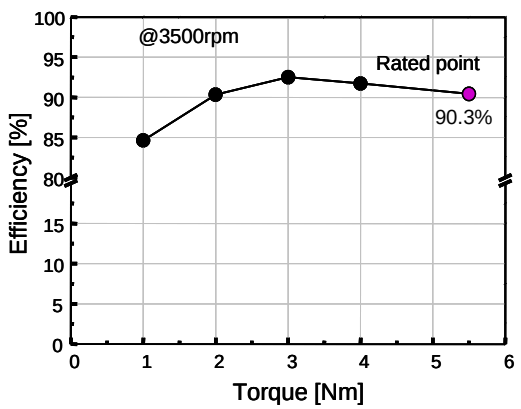

Fig. 16. Efficiency characteristics according to load torque.

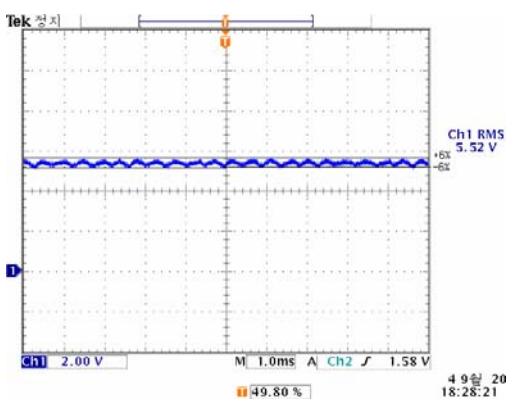

Fig. 17. Torque ripple characteristics at the rated torque (1Nm/V).

5. Conclusions

In this paper, the design result of an IPMSM drive system for the Hybrid Electric Compressor of a HEV operating with a 42V battery system was discussed.

In the driving performance test, the rated driving characteristics and maximum output characteristics are ensured. A high efficiency motor driving characteristic, more than 90%, is achieved, and the test result of the implemented motor drive system is in good agreement with the required specifications.

This system is proposed as a novel technical approach for Hybrid Electric Compressor motor drives.

In the very near future, extensive research will be done considering high voltage (e.g. 180V) motor drive systems in order to reduce motor volume and the current ratings of power switches. Therefore, this system will be a more practical and economical application solution from the viewpoint of the cost reduction of motor drive systems.

Acknowledgment

This work was supported by Kyungnam University Foundation Grant, 2008.

References

[1] Benbouzid, M. E. H. Diallo, D. Zeraoulia, M. Zidani, F. “Active fault-tolerant control of induction motor drives in EV and HEV against sensor failures using a fuzzy decision system,” *International Journal of Automotive Technology*, Vol. 7, pp. 729–739, 2006.

[2] Naidu, M. Henry, R. and Boules, N. “A 3.4 kW, 42 V, high efficiency automotive power generation system,” *Proc. SAE-FTT 2000 Conference*, Vol. 20, pp. 117-120, Aug. 2000.

[3] Murakami, H. Kataoka, H. and Honda, Y. “Highly efficient brushless motor design for an air-conditioner of the next generation 42 V vehicle,” *Proc. IEEE Industry Applications Society Annual Meeting Chicago*, pp. 461-466, 2001.

[4] Oldenkemp, J. L. and Erdman, D. M., “Automotive electrically driven air-conditioning system,” *Int. J. Automotive Power Electronics*, pp. 71-72, Aug. 1989.

[5] Kiekmann, J. and Mallory, D. “Variable speed compressor HFC-134A based air conditioning system for electric

vehicles," *Conference of SAE*. Paper No. 920444, 1992.
[6] Hendershot, J. R. JR, Miller, T. J. E. "Design of Brushless Permanent-Magnet Motors," Magna Physics Publishing and Clarendon Press, pp. 12.2-12.5, 1994.

Tae-Uk Jung was born in Masan, Korea, in 1970. He received a B.S., a M.S. and a Ph.D. in Electrical Engineering from Busan National University, Busan, Korea, in 1993, 1995 and 1999, respectively. Between 1996 and 2005, he was a Chief Research Engineer with the Laboratory of LG Electronics, Korea. Between 2006 and 2007, he was a Senior Research Engineer of the Korea institute of Industrial Technology, Korea. Since 2007, he has been with Kyungnam University as an Assistant Professor. His main research interests are high efficiency motor design, control and applications.